Canadian Journal of Chemistry

Article

Regioselectivity in Wacker oxidations of internal alkenes: antiperiplanar effects?

W.O. Usama[a], **D.J. Markewich**[b], **and A.L.L. East**[c]

[a]Department of Family Medicine, McMaster University, 435 The Boardwalk, Waterloo, ON N2T 0C2, Canada; [b]Department of Pathology and Laboratory Medicine, College of Medicine, University of Saskatchewan, Saskatoon, SK S7N 0W8, Canada; [c]Department of Chemistry and Biochemistry, University of Regina, Regina, SK S4S 0A2, Canada

Corresponding author: **A.L.L. East** (email: allan.east@uregina.ca)

Abstract

Computational chemistry, with considerable effort, was used to elucidate the reason for regioselectivity (12:1 distal:proximal product distribution) in a published Wacker oxidation of internal alkenes with a homoallylic lactam ring. Such a distribution is reproduced by a non-chelating reaction pathway; chelated intermediates are found to be too high in energy. Despite much speculation of chelation effects in the literature, this particular result is most probably an antiperiplanar field effect with no chelation. Partial charge data are provided to support the proposed antiperiplanar effect. The great care needed in modelling Wacker oxidations is emphasized, but optimism is offered that its various product mysteries can be elucidated on a case-by-case basis.

Key words: Wacker, internal alkenes, field effect, through-space effect, product distribution, explicit water, Pd(II) complexes

Résumé

Nous avons utilisé dans un effort considérable la chimie computationnelle pour expliquer la régiosélectivité (distribution distal:proximal 12:1 des produits) observée dans une publication portant sur une oxydation de Wacker d'alcènes internes comportant un cycle lactame homoallylique. Nous sommes parvenus à reproduire une telle distribution par un mécanisme réactionnel non chélatant; les intermédiaires chélatés s'étant révélés trop élevés en énergie. Malgré l'abondance de spéculation concernant les effets de chélation dans la littérature, ce résultat particulier est fort probablement attribuable à un effet de champ antipériplanaire sans chélation. Nous présentons des données de charges partielles pour étayer l'hypothèse de l'effet antipériplanaire. Nous soulignons entre autres le grand soin nécessaire à la modélisation des oxydations de Wacker, tout en faisant preuve d'optimisme quant à la possibilité d'élucider au cas par cas les mystères de la formation des différents produits. [Traduit par la Rédaction]

Mots-clés : Wacker, alcènes internes, effet de champ, effet à travers l'espace, distribution des produits, eau explicite, complexes de Pd(II)

Introduction

In Wacker-type oxidation of alkenes (via homogeneous Pd(II) catalysts), C=O bond formation can in principle occur at either of the olefinic carbon atoms. Any regioselectivity is most likely achieved during the crucial water-addition ("hydroxypalladation") step,[1,2,3a] which occurs while the alkene is coordinated to Pd(II) in a catalytic complex. The regioselectivity can be substrate-controlled (by functional groups already on the alkene) or catalyst-controlled (by use of ligands other than chloride on Pd); the former are of interest here. Sigman has published a large review of Wacker oxidation results, in which he comments on the complexity of the influence of proximal heteroatoms in substrate control of product distribution.[1] Past discussions of substrate-controlled regioselectivity have included commentary (sometimes quite speculative) on whether the control is via chelating,[3] steric,[4] or inductive[5] effects.

For terminal alkenes, regioselectivity generally follows Markovnikov's rule to produce methyl ketones over aldehydes in a >99:1 ratio (and thus the Markovnikov effect is a >3 kcal mol^{-1} effect). There are published cases of anti-Markovnikov Wacker distributions that favour aldehydes (by accident or by design);[6] these cases must therefore possess a significant (>3 kcal mol^{-1}) counteracting effect, due perhaps to steric crowding or to ring strain caused by chelation. However, for internal 1,2-disubstituted alkenes, which have no governing Markovnikov effect, regioselectivity can be achieved with very small effects (e.g., a 1.4 kcal mol^{-1} effect would produce a 10:1 product distribution at 300 K), where inductive or field effects might be sufficient.[5] Several

Fig. 1. Wacker oxidation of 1,2-substituted alkenes featuring proximal lactam rings, performed at [Cl^-] < 1 mol/L conditions.[8]

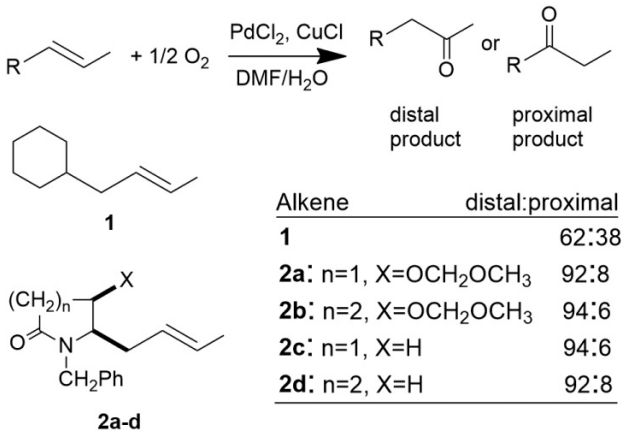

Alkene	distal:proximal
1	62:38
2a: n=1, X=OCH_2OCH_3	92:8
2b: n=2, X=OCH_2OCH_3	94:6
2c: n=1, X=H	94:6
2d: n=2, X=H	92:8

cases of regioselectivity with internal alkenes are known but are not well understood.[1] Here, we investigate, using DFT (density functional theory) computation,[7] one particular case of regioselectivity from an internal alkene, and give evidence for a field effect.

The case we investigated came from a laboratory down the hall from us. Annadi and Wee[8] reported syntheses of spirolactams that benefitted from unexpected regioselectivity of Wacker oxidation of internal alkenes possessing a lactam group with a homoallylic N atom (Fig. 1). To probe the reasons for their ~12:1 distal:proximal regioselectivity, they performed more oxidations of alkenes, both internal and terminal, with and without the lactam group. Although they concluded that their extra data were suggestive of a chelation effect (proposed to be Pd→N coordination), this is incorrect. Their extra work sheds no light on the reason for the lactam effect; it only serves to demonstrate that a lactam effect exists (even upon terminal alkene oxidation, although the inherent Markovnikov regioselectivity still dominated).[8] We note that 40 years ago Tsuji found a similar 10:1 distal:proximal product distribution from an internal alkene, having a homoallylic bridging O in an ester group,[9] and he also chose to offer chelation as the possible reason. This short article is intended to serve notice that simple electronic (inductive or field) effects should not be overlooked in Wacker oxidation of internal alkenes.

Computational methods

The Gaussian09 software[7b] was used. Calculations used the B3LYP approximation of DFT[7c,7d] and the default self-consistent reaction field continuum-solvation model (SCRF CSM)[10] in Gaussian09. The default SCRF CSM, as described by Scalmani and Frisch,[10a] is the 2002 polarizable continuum model of Cossi, Scalmani, Rega, and Barone,[10b] but with a solute cavity surface discretization scheme of Scalmani and Frisch, which they termed the continuous surface charge formalism[10a] (extending on an idea of York and Karplus[10c]). The solute cavity surface is an overlapping-spheres van-der-Waals surface (not a solvent-excluded surface), using United Force Field (UFF) atomic radii[10d] scaled by default by a factor of 1.1 to reasonably mimic cavity volumes from an earlier solvent-excluded-surface definition.[10a]

Fig. 2. B3LYP/SDD/SCRF (self-consistent reaction field) results, using a rule that no solvent H_2O molecules be allowed to H-bond to each other. The true value is roughly 2–5 kcal mol^{-1}, estimated from the experimentally determined zero-ionic-strength equilibrium constant[19] of $10^{0.9}$ (20 °C) for the reverse reaction, which assumes [H_2O] = 55.45 mol/L: $\Delta E_{elec} \approx \Delta G([H_2O] = 1\ mol/L) = +RT\ ln\ (55.45 * 10^{0.9}) = +3.6$ kcal mol^{-1}.

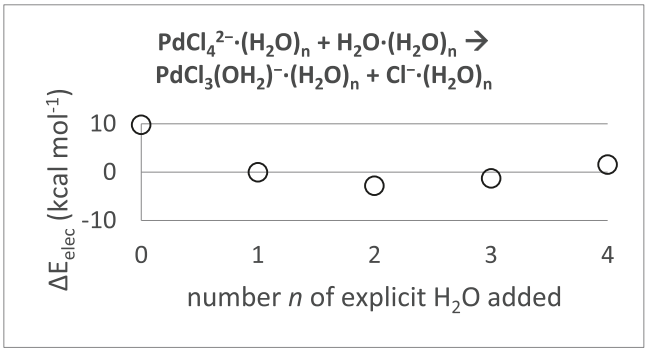

The semicontinuum testing work (vide infra) used the SDD[11] basis set throughout (i.e., B3LYP/SDD/SCRF), while the remainder used B3LYP/TZP/SCRF single points at B3LYP/DZP/SCRF geometries: here, DZP is defined to be SDD on Pd and 6-31G(d,p)[7b] on all other atoms, while TZP is defined to be SDD(f)[12] on Pd and 6-311+G(2d,p)[7b] on all other atoms. The 6-31G(d,p) basis was employed with spherical-harmonic 5d sets, not Cartesian 6d sets as was originally defined.[7b] Transition-state geometry optimizations were also performed, and the elementary step involved was confirmed via normal geometry optimizations begun from +/− displaced geometries on either side of the transition state. All computed Gibbs energies have standard-state concentration corrections $-RT\ ln\ V^*/V^\circ$ applied post-calculation: +1.9 kcal mol^{-1} for solutes (V^*/V° = 1/24.466 for 1 atm → 1 mol/L), but +4.3 kcal mol^{-1} for liquid water when a reactant (V^*/V° = 0.018/24.466 for 1 atm → 55.45 mol/L). Note that Gibbs energy estimates will have more error than electronic energies and enthalpies, due to additional error in harmonic-oscillator entropies,[13] and results from electronic energies alone will also be presented. Partial charges were computed using a Natural Bond Order[14] analysis.

Computational modelling of Wacker oxidations requires great care. First, the reaction has a complex and not-fully-elucidated multistep mechanism that is sensitive to the concentrations of chloride and copper present.[15] Second, the Sigman review[1] suggests to us that chelation by an alkene substituent may or may not occur, depending on heteroatom basicity and ring strain. Third, there is debate on whether the water molecule supplying the O atom is initially coordinated to Pd ("inner-sphere" syn addition)[15] or not ("outer-sphere" anti-addition),[16] and whether this is dependent on conditions. Fourth, ab initio or DFT computations of Wacker

Fig. 3. Placement of explicit water molecules for comparing relative energies of possible π complexes of alkene **2e** (similar to **2d**, but with CH_2Ph replaced by CH_3 for computational feasibility). [Colour online.]

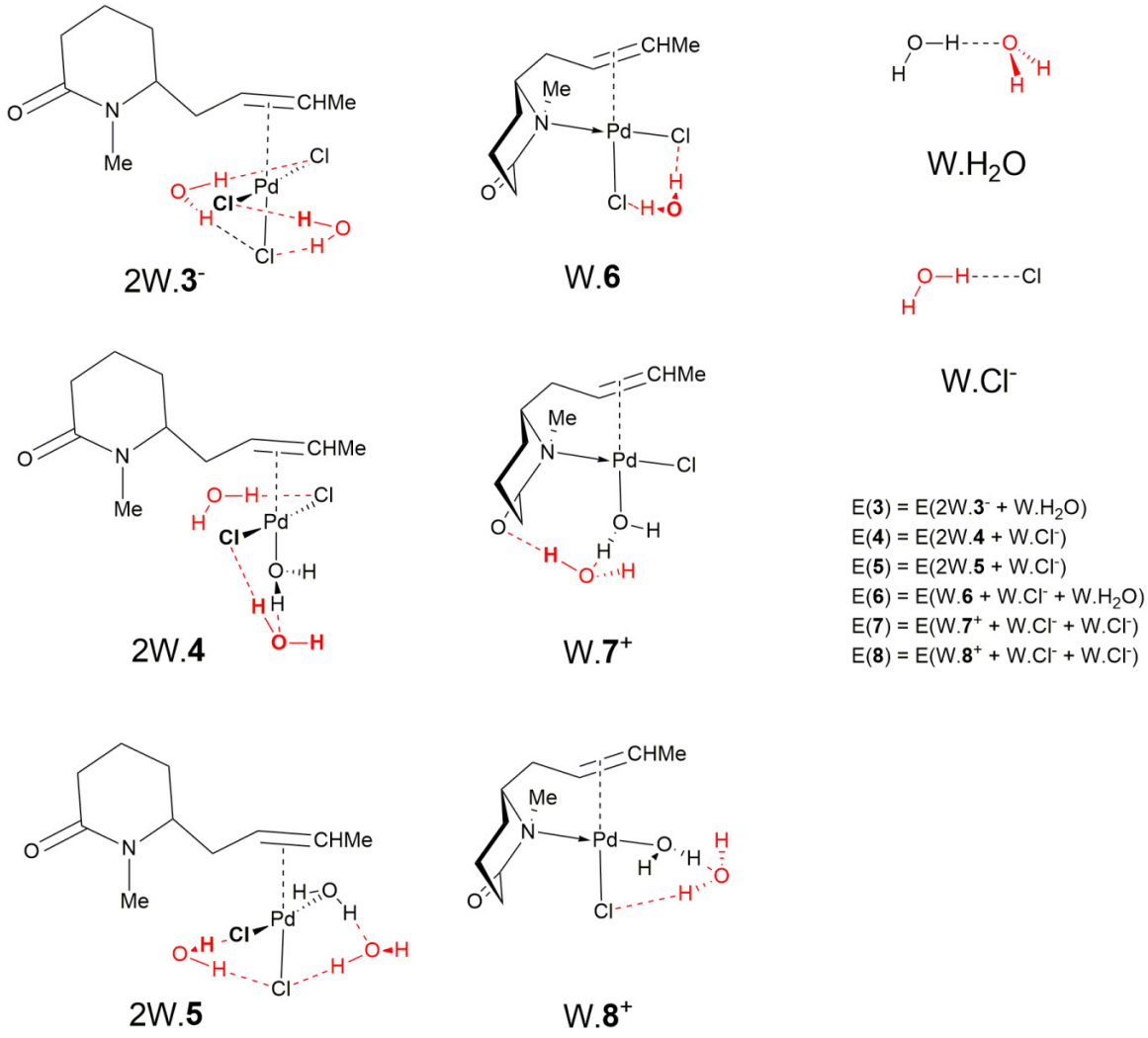

Table 1. Relative B3LYP/SCRF (self-consistent reaction field) energies (kcal mol^{-1}) of hypothetical π complexes of **2e** (Fig. 3).

Version[a]	E_{rel} (DZP)	E_{rel} (TZP)	H_{rel}[b]	G_{rel}[b]
2W.**3**$^{-}$ · + W.H_2O	0.0	0.0	0.0	0.0
2W.**4**· + W.Cl^{-}	0.6	2.1	2.6	2.9
2W.**5**· + W.Cl^{-}	2.0	4.4	4.9	5.1
W.**6** + W.H_2O + W.Cl^{-}	24.0	17.7	16.4	10.7
W.**7**$^{+}$ + 2 W.Cl^{-}	26.6	22.6	21.6	16.2
W.**8**$^{+}$ + 2 W.Cl^{-}	28.2	23.9	23.1	17.4

[a]W = explicit spectator water molecule.
[b]From adding B3LYP/DZP/SCRF thermal corrections to B3LYP/TZP/SCRF E_{rel} values. G_{rel} includes concentration corrections (see Methods).

oxidations are further hampered by inherent difficulties in modelling aqueous-phase reactions involving H bonding or proton transfer with solvent; note that the Goddard group invoked corrections of 16 kcal mol^{-1} in their modelling of the Wacker mechanism.[15a] Fifth, care is needed in determining lowest energy conformers of possible intermediates, as conformer effects could easily be larger than the 1.5 kcal mol^{-1} effect one is attempting to see (from an observed 12:1 product distribution).

We used a semicontinuum modelling technique[17] for improved accuracy for aqueous ions. This technique, also called the cluster + continuum technique,[18] adds explicit water molecules around the solute molecule as well as a dielectric continuum field having the polarity of water. Here, initial testing on a ligand-interchange reaction of $PdCl_4^{2-}$ (Fig. 2; $\Delta E_{elec,\ expt} \approx$ 2–5 kcal mol^{-1} from experiment[19]) showed the importance of adding explicit water: in this reaction, a 6 kcal mol^{-1} error is made by $n = 0$ modelling (i.e., neglecting explicit H_2O). This large error is due to neglecting particularly strong H-bond stabilization of $PdCl_3(OH_2)^{-}$ by solvent water. Such modelling is also important for reactions involving production or consumption of H_3O^{+},[20,21] which would include hydroxypalladation here.

The semicontinuum technique was applied as follows. For the π-complex comparisons (**3–8**, Fig. 3), three water molecules were added: 1 to solvate H_2O and 2 to solvate vari-

Fig. 4. The inner-sphere hydroxypalladation step. [Colour online.]

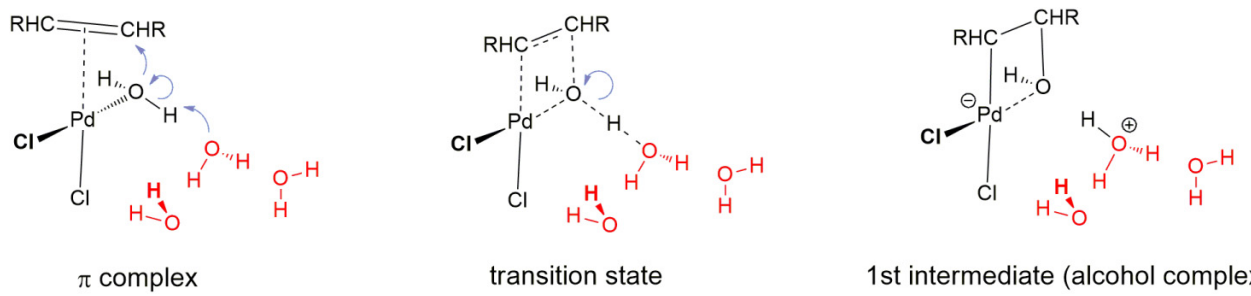

Fig. 5. Reaction energy profiles from DFT (density functional theory) calculations for the inner-sphere hydroxypalladation step in the Wacker oxidation of **1** and **2** (using **2e** for **2**), starting from non-chelated π-complex **5** of Fig. 2, i.e., **5(1)** or **5(2)**. Upper and lower left: transition-state energies ($\Delta^{\ddagger}E_{elec}$, $\Delta^{\ddagger}G$). Upper and lower right: reaction energies (ΔE_{elec}, ΔG). The splittings highlighted in the figure match well the experimental splittings of 1.5 (lactam) and 0.3 (cyclohexyl), proving that such splittings can be obtained from electronic effects. The insensitivity of the energy splitting of intermediates to H_2O placement was confirmed by a parallel calculation of the lactam-case splitting using no explicit waters, duplicating the 1.4 kcal mol^{-1} result in the upper right plot.

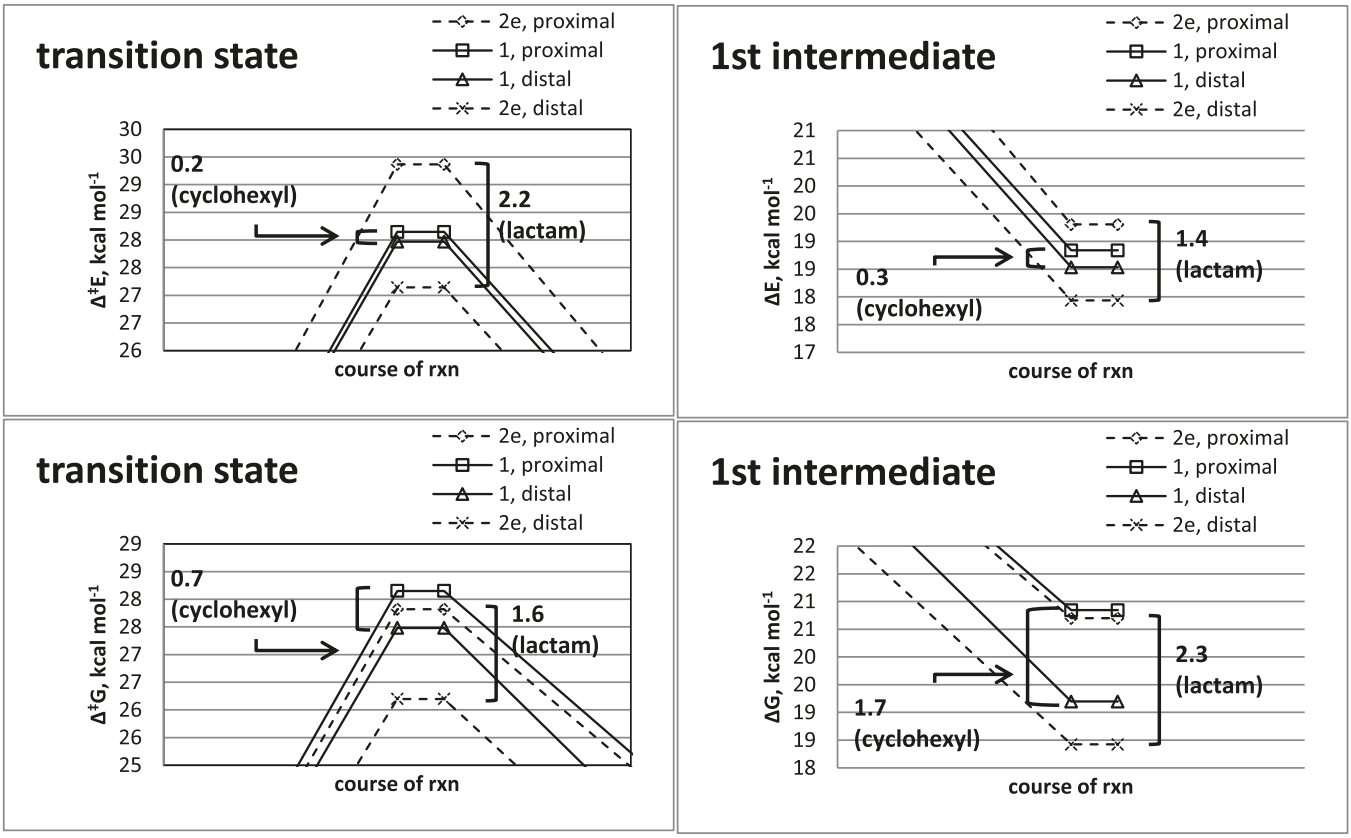

ous Cl$^-$. For instance, for E(**5**), we used E(2W.**5**) + E(W.Cl$^-$), while for E(**6**), we used E(W.**6**) + E(W.H_2O) + E(W.Cl$^-$), each complex computed in a surrounding continuum dielectric (SCRF PCM) for effects of bulk aqueous solvent. In testing, we found that it is crucial to be consistent with the number of OH…O H-bonds between the O of an explicit (spectator) W and an H of the H_2O molecule involved in complexation/decomplexation. Hence, in each case (**3–8**), we ensured that there was only one such OH…O H-bond. For the hydroxypalladation step, a different placement of the three explicit water molecules was used (vide infra) to somewhat realistically solvate the ejected H$^+$, while maintaining a constant number of OH…O H-bonds and OH…Cl$^-$ ion–dipole interactions from reactant to first intermediate.

Results and discussion

First, we give evidence that chelation with **2a–2d** is unlikely. Using **2e** (a modified **2d**, with CH_2Ph replaced by CH_3

for computational feasibility),[22] we determined the relative energies of several hypothetical versions (**3–8**,Fig. 2) of the Pd·alkene π-complex intermediate that would serve as the starting point for the water-addition step. (Chelation via the carbonyl oxygen is not sterically possible.) These calculations were not trivial, requiring not only semicontinuum modelling but also careful conformer searches (Supplementary Material). Once these calculations were complete, the energy predictions (Table 1) place the chelating structures **6–8** too high in energy to occur. The homoallylic amide nitrogen is not sufficiently basic to afford chelation.

Given the interest in substrate control of Wacker regioselectivity via chelation, this weak Pd–N interaction with the lactam **2e** was compared to Pd–O interactions in lactone and ring-ether analogues of **2e**. Values for this chelation interaction energy were computed as 2W.**5** → W.**6** + W.H_2O (i.e., negative energies indicating stabilization): the values were +13.3 for the lactam, +14.5 for the lactone, and +2.4 for the ring-ether. Subtracting from each value a crude 4 kcal mol^{-1} for the entropy benefit of chelation, the only plausible homoallylic chelation interaction of the three is in the ring-ether case.

Second, we show that the lactam effect (the product distributions seen with both **1** and **2**) is reproduced, without invoking chelation, by DFT calculations on the hydroxypalladation step. Restricting attention to the energetically viable cases **3–5**, and guided by the conclusion of Henry and co-workers that the water addition is inner-sphere under low-chloride conditions,[15] we took the lowest energy conformer of **5** (since **3** and **4** cannot perform this step), and obtained transition states and the ensuing first intermediates for both proximal and distal inner-sphere addition (Fig. 4). Note the use of three explicit H_2O molecules for the historically challenging job of adequately stabilizing aqueous H^+ in such reaction steps. The resulting energies are plotted in Fig. 5, with the proximal–distal splittings highlighted. The $\Delta^{\ddagger}E$ or $\Delta^{\ddagger}G$ (activation) comparisons would be relevant if the reaction were kinetically controlled; the ΔE or ΔG (reaction) comparisons would be relevant if the reaction were thermodynamically controlled. The known product ratios of [distal]/[proximal] = 62/38 and 92/8 (Fig. 1), inserted into the relation δE = RT ln([distal]/[proximal]), correspond to energy splittings of δE = 0.3 and 1.5 kcal mol^{-1} for **1** and **2**, respectively. These splittings from experiment are reproduced very well by the predictions in Fig. 5. The most precise of the predictions in Fig. 5 would be the upper right plot of electronic reaction energies; B3LYP is expected to be less accurate for transition states[23] (upper left plot), and terms for Gibbs energies (lower right plot) also introduce some imprecision. In this regard, the Gibbs activation energies, $\Delta^{\ddagger}G$ (lower left plot), were perhaps fortuitous in reproducing the experimental splittings well. Now, since the structures used possess no chelation and reveal no obvious steric effects, the lactam effect displayed by the calculations must be due to an electronic effect. This completes the demonstration that an electronic effect can be the reason behind the lactam effect observed experimentally.

Third, we explore the nature of the electronic effect causing the splittings produced by the DFT predictions. In the

Fig. 6. Proposed antiperiplanar field effect: electrostatic forces between C_β and C_{prox}. Hollow arrows indicate bond dipoles inducing partial charges. Red and blue indicate positive and negative partial charges, respectively (as seen in partial-charge calculations; see Supplementary Material). [Colour online.]

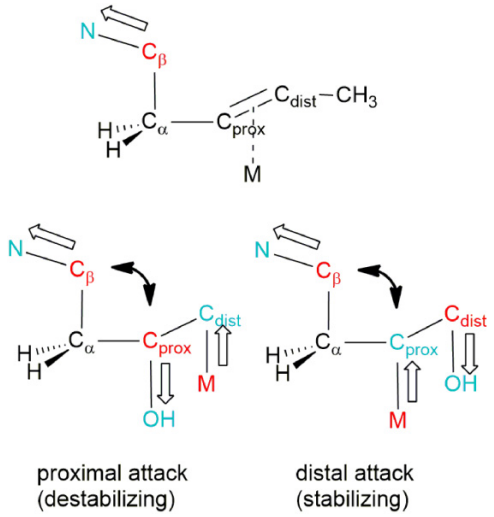

π-complex **5**, partial-charge and LUMO calculations show no regioselective effects: the lactam group has a short-range effect that does not reach past the methylene group. Regioselectivity from the DFT calculations is occurring once covalent bonds from Pd and O begin to form with the C=C entity, creating partial charges on both these C atoms. As Fig. 6 suggests, proximal attack of water creates, among other new electrostatic interactions, a C_β–C_{prox} field-effect (through-space) repulsion, while distal attack of water creates a C_β–C_{prox} field-effect attraction, and we propose (based on an analysis of Natural Bond Orbital[14] partial charges; see Supplementary Material) that these are the dominant destabilizing and stabilizing effects occurring with the lactam group. The cyclohexyl group (see **1** in Fig. 1) has virtually no partial charge at C_β, resulting in virtually no C_β–C_{prox} effects and hence virtually no regioselectivity. Furthermore, this lactam field effect can be termed an antiperiplanar effect, since if the C_β were not antiperiplanar with the group X (M or OH) causing C_{prox} to be charged, the C_β–C_{prox} interaction would be offset by the strengthened C_β–X interaction. In our test calculations, these abovementioned net effects appear to be significantly dependent on the magnitudes of the partial charges involved, and as such may not be generalizable.

In summary, computational chemistry was able to nearly quantitatively reproduce the 12:1 distal:proximal product distribution observed in Wacker oxidation of alkenes **2a–2d**, all featuring a homoallylic N atom in a lactam ring. The 1.5 kcal mol^{-1} effect was reproduced by an electronic effect, rather than a chelating effect, and an argument for an antiperiplanar field effect (a through-space C_β–C_{prox} interaction, due to created partial charge on C_β) is proposed. Practition-

ers should be cautious of chelation conjectures for effects of ~1.5 kcal mol^{-1} in Wacker oxidations.

Acknowledgements

The work was supported by the Natural Sciences and Engineering Research Council (Discovery Grant 238871-2012) and the Canada Foundation for Innovation (Leading Edge Fund 2009, grant 21625). A.G.H. Wee is thanked for proposing the investigation of this regioselectivity. We also thank K. Annadi and A. Jayaraman for useful discussions, L. Hoffert for exploratory calculations on some terminal alkene cases, and A. Nicolaides (University of Cyprus) for a discussion of possible negative hyperconjugation. We especially thank S. Rayne for his 2015 work with ALLE in developing semicontinuum models, generating the data for Fig. 2 and initial models for Wacker π complexes.

Article information

History dates

Received: 15 June 2022
Accepted: 25 August 2022
Accepted manuscript online: 1 September 2022
Version of record online: 27 October 2022

Notes

This paper is one of a selection of papers from the 12th Triennial Congress of the World Association of Theoretical and Computational Chemists (WATOC 2020).

Copyright

Data availability

Data generated during this study are available from the corresponding author upon reasonable request.

Author information

Author ORCIDs

A.L.L. East https://orcid.org/0000-0003-1898-4370

Competing interests

The authors declare there are no competing interests.

Supplementary material

Supplementary data are available with the article at https://doi.org/10.1139/CJC-2022-0151 and include details regarding orbital basis sets, conformer searches, post-justification of use of **2e**, partial charge analysis, and Cartesian coordinates of all reported structures.

References

(1) Michel, B. W.; Steffens, L. D.; Sigman, M. S. Org. React. **2014**, *84*, 75.
(2) McDonald, R. I.; Liu, G.; Stahl, S. S. Chem. Rev. **2011**, *111*, 2981. doi:10.1021/cr100371y.
(3) (a) Dong, J. J.; Browne, W. R.; Feringa, B. L. Angew. Chem., Int. Ed. **2015**, *54*, 734. doi:10.1002/anie.201404856;(b) Muzart, J. Tetrahedron, **2007**, *63*, 7505. doi:10.1016/j.tet.2007.04.001.
(4) Majik, M. S.; Tilve, S. G. Tetrahedron Lett. **2010**, *51*, 2900. doi:10.1016/j.tetlet.2010.03.098.
(5) (a) Morandi, B.; Wickens, Z. K.; Grubbs, R. H. Angew. Chem., Int. Ed. **2013**, *52*, 9751. doi:10.1002/anie.201303587;(b) Lerch, M. M.; Morandi, B.; Wickens, Z. K.; Grubbs, R. H. Angew. Chem., Int. Ed. **2014**, *53*, 8654. doi:10.1002/anie.201404712.
(6) (a) Krishnudu, K.; Krishna, P. R.; Mereyala, H. B. Tetrahedron Lett. **1996**, *37*, 6007. doi:10.1016/0040-4039(96)01261-0;(b) Weiner, B.; Baeza, A.; Jerphagnon, T.; Feringa, B. L. J. Am. Chem. Soc. **2009**, *131*, 9473. doi:10.1021/ja902591g;(c) Choi, P. J.; Sperry, J.; Brimble, M. A. J. Org. Chem. **2010**, *75*, 7388. doi:10.1021/jo1016585.
(7) (a) Gaussian09 software7b was used. Calculations used the B3LYP approximation of density functional theory7c,d and the default self-consistent reaction field (SCRF)7e solvent continuum approximation in Gaussian09. For full details see Supplementary Material;(b) Frisch, M. J., et al. Gaussian09, Rev. C.01. Gaussian, Inc.: Wallingford CT, **2009**;(c) Becke, A. D. J. Chem. Phys. **1993**, *98*, 5648. doi:10.1063/1.464913;(d) Lee, C.; Yang, W.; Parr, R. G. Phys. Rev. B, **1988**, *37*, 785. doi:10.1103/PhysRevB.37.785;(e) Tomasi, J.; Mennucci, B.; Cammi, R. Chem. Rev. **2005**, *105*, 2999. doi:10.1021/cr9904009.
(8) Annadi, K.; Wee, A. G. H. J. Org. Chem. **2016**, *81*, 1021. doi:10.1021/acs.joc.5b02582.
(9) Tsuji, J.; Nagashima, H.; Hori, K. Tetrahedron Lett. **1982**, *23*, 2679. doi:10.1016/S0040-4039(00)87430-4.
(10) (a) Scalmani, G.; Frisch, M. J. J. Chem. Phys. **2010**, *132*, 114110. doi:10.1063/1.3359469;(b) Cossi, M.; Scalmani, G.; Rega, N.; Barone, V. J. Chem. Phys. **2002**, *117*, 43. doi:10.1063/1.1480445;(c) York, D. M.; Karplus, M. J. Phys. Chem. A, **1999**, *103*, 11060. doi:10.1021/jp992097l;(d) Rappé, A. K.; Casewit, C. J.; Colwell, K. S.; Goddard, W. A., III; Skiff, W. M. J. Am. Chem. Soc. **1992**, *114*, 10024. doi:10.1021/ja00051a040.
(11) Andrae, D.; Haeussermann, U.; Dolg, M.; Stoll, H.; Preuss, H. Theor. Chem. Acc. **1990**, *77*, 123. doi:10.1007/BF01114537.
(12) Ehlers, A. W.; Böhme, M.; Dapprich, S.; Gobbi, A.; Höllwarth, A.; Jonas, V.; Köhler, K. F.; Stegmann, R.; Veldkamp, A.; Frenking, G. Chem. Phys. Lett. **1993**, *208*, 111. doi:10.1016/0009-2614(93)80086-5.
(13) East, A. L. L.; Radom, L. J. Chem. Phys. **1997**, *106*, 6655. doi:10.1063/1.473958.
(14) Reed, A. E.; Weinstock, R. B.; Weinhold, F. J. Chem. Phys. **1985**, *83*, 735. doi:10.1063/1.449486.
(15) (a) Keith, J. A.; Nielsen, R. J.; Oxgaard, J.; Goddard, W. A. , III J. Am. Chem. Soc. **2007**, *129*, 12342. doi:10.1021/ja072400t;(b) Keith, J. A.; Nielsen, R. J.; Oxgaard, J.; Goddard, W. A., III; Henry, P. M. Organometallics, **2009**, *28*, 1618. doi:10.1021/om800013p;(c) Keith, J. A.; Henry, P. M. Angew. Chem., Int. Ed. **2009**, *48*, 9038. doi:10.1002/anie.200902194;(d) Outer-sphere attack of 3–5 might also give similar agreement with experiment, but such calculations would need to investigate a very large set of conformer possibilities.
(16) (a) Kovács, G.; Stirling, A.; Lledós, A.; Ujaque, G. Chem. - Eur. J. **2012**, *18*, 5612. doi:10.1002/chem.201102138;(b) Stirling, A.; Nair, N. N.; Lledós, A.; Ujaque, G. Chem. Soc. Rev. **2014**, *43*, 4940. doi:10.1039/C3CS60469A;(c) Imandi, V.; Nair, N. N. J. Phys. Chem. B, **2015**, *119*, 11176. doi:10.1021/acs.jpcb.5b03099;(d) Kočovský, P.; Bäckvall, J.-E. Chem. - Eur. J. **2015**, *21*, 36. doi:10.1002/chem.201404070.
(17) (a) Rick, S. W.; Berne, B. J. J. Am. Chem. Soc. **1994**, *116*, 3949. doi:10.1021/ja00088a034;(b) Sumon, K. Z.; Bains, C. H.; Markewich, D. J.; Henni, A.; East, A. L. L. J. Phys. Chem. B, **2015**, *119*, 12256. doi:10.1021/acs.jpcb.5b06076.
(18) Pliego, J. R., Jr.; Riveros, J. M. J. Phys. Chem. A, **2001**, *105*, 7241. doi:10.1021/jp004192w.
(19) Boily, J.-F.; Seward, T. M. Geochim. Cosmochim. Acta, **2005**, *69*, 3773. doi:10.1016/j.gca.2005.03.015.
(20) Dhillon, S.; East, A. L. L. Int. J. Quantum Chem. **2018**, *118*, e27503. doi:10.1002/qua.25703.
(21) Patel, D. H.; East, A. L. L. J. Phys. Chem. A, **2020**, *124*, 9088. doi:10.1021/acs.jpca.0c07011.
(22) The replacement of N-CH_2Ph with N-Me was post-justified to be accurate; see p. S8 of Supplementary Material.
(23) Ess, D. H.; Houk, K. N. J. Phys. Chem. A, **2005**, *109*, 9542. doi:10.1021/jp052504v.